Structural Investigation of Palladium Clusters on γ-AlO₃(111)/NiAl(110) with Transmission Electron Microscopy

S. A. Nepijko,[†] M. Klimenkov,[†] M. Adelt,[†] H. Kuhlenbeck,*,[†] R. Schlögl,[‡] and
H.-J. Freund[†]

Abteilung Chemische Physik and Abteilung Anorganische Chemie, Fritz-Haber-Institut der Max-Planck-Gesellschaft, Faradayweg 4-6, D-14195 Berlin, Germany

For Pd clusters on γ-Al₂O₃ epitaxially grown on NiAl(110) the lattice constant has been determined as a function of the cluster size by evaluating patterns induced by double diffraction involving the NiAl substrate and the cluster lattice. Similar to results reported previously for platinum and tantalum clusters on the same substrate (*Surf. Sci.* **1997,** *391,* 27; *Surf. Sci.* **1998,** *413,* 192), we observe a reduction of the distances within the lattice with decreasing cluster size. The highest observed reduction is 5% for clusters with a diameter of about 12 Å. Within the limits of the experimental errors the reduction of the lattice distances is isotropic. Although the samples have been exposed to air prior to investigation, the clusters are only weakly oxidized as concluded from XPS data.

Introduction

It is well-known that deposited clusters exhibit size dependent lattice constants,[3] which may be traced back to the influence of the cluster−vacuum and the cluster−substrate interface. Since the electronic structure of clusters depends, apart from other parameters, on the distances within the lattice, size-dependent adsorption properties result. This effect is of technical importance since in catalysis deposited metal clusters play an important role as active parts of catalysts. Recently we have studied adsorption on Pd and Pt clusters on γ-Al₂O₃/NiAl(110) under UHV (ultrahigh vacuum) conditions using photoelectron and infrared spectroscopy.[4−6] Adsorption properties strongly different from those of the bulk material were observed in both cases. For instance, platinum clusters were found to exhibit a pronounced tendency for CO dissociation[4] which is not the case for bulk samples.

Previously we have investigated tantalum and platinum clusters deposited on γ-Al₂O₃(111)/NiAl(110)[1,2] with transmission electron microscopy (TEM). For both materials we found that the lattice constant decreased with decreasing cluster size. This is in agreement with theory for platinum,[7] whereas for tantalum no theoretical results exist. For palladium, theoretical studies predict a decrease

of the lattice constant with decreasing cluster size.[8−11] However, no significant dependence of the lattice constant on the cluster size,[12] as well as an increasing lattice constant,[13] has been found in experimental studies. These results were obtained using methods integrating over a certain area of the substrate surface so that they refer to an ensemble of clusters with a certain spread of sizes. Transmission electron microscopy on the other hand permits to study individual clusters so that this method is well suited to investigate the cluster size/lattice constant relationship of deposited particles in detail.

Recent studies with STM (scanning tunneling microscopy) under UHV conditions have demonstrated that the shapes of Pd and Pt particles on /NiAl(110) are different: platinum clusters are flatter than palladium clusters.[14,15] This means that the bonding of platinum to the substrate is most likely stronger than that of palladium since a stronger interaction favors a larger oxide/substrate contact area. Since the cluster/substrate interaction may also be important for the interatomic spacing in small particles, different cluster size/lattice constant relationships for palladium and platinum may result.

Experimental Section

γ-Al₂O₃ films have been prepared by oxidation of a NiAl(110) single-crystal disk with a thickness of about 0.3 mm and 3 mm diameter. The substrate has been cut off of a single-crystal rod after orientation with Laue backscattering with an accuracy of about ±1°. After the disk was polished using standard procedures, it was etched in a fast ion etching system until a hole with a diameter of about 0.2 mm was formed in the center (see Figure

* Corresponding author: Telephone: +49 30 8413 4222. Fax: +49 30 8413 4307. E-mail: Kuhlenbeck@FHI-Berlin.MPG.DE.
† Abteilung Chemische Physik.
‡ Abteilung Anorganische Chemie.

(1) Klimenkov, M.; Nepijko, S.; Kuhlenbeck, H.; Bäumer, M.; Schlögl, R.; Freund, H.-J. *Surf. Sci.* **1997,** *391,* 27.
(2) Nepijko, S. A.; Klimenkov, M.; Kuhlenbeck, H.; Zemlyanov, D.; Herein, D.; Schlögl, R.; Freund, H.-J. *Surf. Sci.* **1998,** *413,* 192.
(3) Boswell, F. W. C. *Proc. Phys. Soc. A* **1951,** *64,* 465.
(4) Wohlrab, S.; Winkelmann, F.; Kuhlenbeck, H.; Freund, H.-J. Adsorption on Epitaxial Oxide Systems as Model Systems for Heterogeneous Catalysis. In *Surface Science: Principles and Current Applications;* McDonald, R. J., Taglauer, E. C., Wandelt, K., Eds.; Springer Verlag: Berlin, Germany, 1996.
(5) Wolter, K.; Seiferth, O.; Libuda, J.; Kuhlenbeck, H.; Bäumer, M.; Freund, H.-J. *Surf. Sci.* **1997,** in press.
(6) Wolter, K.; Seiferth, O.; Kuhlenbeck, H.; Bäumer, M.; Freund, H.-J. *Surf. Sci.* **1998,** *399,* 190.
(7) Khana, S. N.; Bucher, J. P.; Buttet, J.; Cyrot-Lackmann, F. *Surf. Sci.* **1983,** *127,* 165.

(8) Silva, E. Z. D.; Antonelli, A. *Phys. Rev. B* **1996,** *54,* 17057.
(9) Fritsche, H.-G. *Z. Phys. Chem.* **1995,** *191,* 219.
(10) Fritsche, H.-G. *Z. Phys. Chem.* **1995,** *192,* 21.
(11) Krüger, S.; Vent, S.; Rösch, N. *Ber. Bunsen-Ges. Phys. Chem. Int. Ed.* **1997,** *101,* 1640.
(12) Oschima, K.; Harada, J. *J. Phys. C: Solid State Phys.* **1984,** *17,* 1607.
(13) Goyhenex, C.; Henry, C. R.; Urban, J. *J. Philos. Mag. A* **1994,** *69,* 1073.
(14) Bäumer, M.; Libuda, J.; Freund, H.-J.; Graw, G.; Bertrams, T.; Neddermeyer, H. *Ber. Bunsen-Ges. Phys. Chem.* **1995,** *99,* 1181.
(15) Libuda, J.; Winkelmann, F.; Bäumer, M.; Freund, H.-J.; Bertrams, T.; Neddermeyer, H.; Müller, K. *Surf. Sci.* **1994,** *318,* 112.
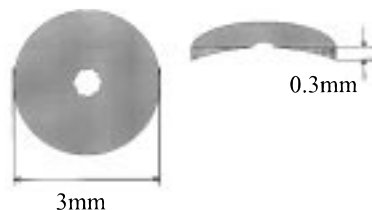
Figure 1. Sample setup used for the experiments.

1). The edge of the hole was wedge shaped with an angle of $5-10°$ and a thickness of less than 10 Å directly at its boundary, thus permitting transmission electron microscopy to be performed in the region near to the hole.

Preparation of the sample, oxidation, and cluster deposition were performed in a simple UHV system with a base pressure of about 10^{-10} mbar. It was equipped with facilities for sample preparation and a LEED system for analysis of surface order. The sample was mounted between two strips of tantalum foil. Heating was possible by passing an electric current through the strips. The samples were cleaned in UHV by repeated cycles of sputtering with Ar ions (700 eV) at room temperature and annealing at 1300 K. After cleaning and ordering, the oxide film was prepared by dosing oxygen (1500 L at 5×10^{-6} mbar) with the sample temperature held at 550 K followed by annealing for some minutes at 1200 K. The oxide film is about 5 Å thick, is well ordered, and exhibits a complicated LEED pattern. More details of the preparation procedure and the structure of the film may be found in refs 16−18.

Palladium clusters were deposited onto the film by thermal evaporation with a flux of 1 Å/min. During deposition the sample was held at room temperature. The flux of the evaporator was calibrated using a quartz microbalance, and the amount of deposited palladium was determined by multiplying the flux by the deposition time.

For the studies two different 200 keV electron microscopes (Hitachi-8100 and Philips CM-200FEG; ultimate lattice resolution in both cases 1.44 Å) containing facilities for energy-dispersive X-ray spectroscopy (EDX) and electron energy loss spectroscopy (EELS), respectively, were used. The double tilt specimen holders of the microscopes allowed for precise positioning and alignment of the sample with respect to the electron beam. During the transfer from the UHV system into the microscope the samples were exposed to air for a few minutes.

XPS (X-ray photoelectron spectroscopy) data have been taken in a modified Leybold LHS 12 system with MCD (multichannel) detection and facilities for XPS and ISS (ion scattering spectroscopy). Electrons have been excited with Mg Kα radiation ($h\nu$ = 1253.6 eV). For the XPS experiments the analyzer pass energy was set to 108 eV, corresponding to an energy resolution of about 1.2 eV.

Results and Discussion

Structure of the Pd clusters Palladium Clusters.
Palladium clusters on γ-Al$_2$O$_3$/NiAl(110) produce only a small contrast in TEM images so that the lattice cannot be studied directly. However, when the experimental conditions are chosen appropriately, moiré fringes show up in the TEM images which can be exploited to get information on the lattice structure.[1,18] The intensity of the moiré fringes depends strongly on the incidence angle of the electron beam with respect to the sample. Fringes with high contrast will show up under conditions when the diffracted beams that generate the fringes are strong and the other ones are weak. The first condition opens up the possibility to chose different sets of moiré fringes by varying the electron incidence angle. For dark- or bright-

(16) Jaeger, R. M.; Kuhlenbeck, H.; Freund, H.-J.; Wuttig, M.; Hoffmann, W.; Franchy, R.; Ibach, H. *Surf. Sci.* **1991**, *259*, 235.

(17) Libuda, J.; Bäumer, M.; Freund, H.-J.; Bertrams, T.; Neddermeyer, H.; Müller, K. *Surf. Sci.* **1994**, *318*, 61.

(18) Klimenkov, M.; Nepijko, S.; Kuhlenbeck, H.; Freund, H.-J. *Surf. Sci.* **1997**, *385*, 66.

Table 1. List of Moiré Types Observed in Parts a and b of Figure 3

type	visible in figure 3	NiAl reciprocal lattice vector	Pd reciprocal lattice vector	eq for the calculation of the Pd lattice constant a
1	a	111 type	220 type	$a = \sqrt{3}a_{111} = \sqrt{3}/|\vec{k}_{111}|$
2	c	110 type	200 type	$a = 2a_{200} = 2/|\vec{k}_{200}|$
3	c	110 type	111 type	$a = \sqrt{8}a_{220} = \sqrt{8}/|\vec{k}_{220}|$

field images, the second condition would be fulfilled best. However, in such images usually the substrate lattice is invisible, prohibiting calibration of the length scale.

The electron diffraction pattern displayed in Figure 2a has been taken with the electron beam penetrating the sample along a direction near to the surface normal (NiAl[110]) whereas for Figure 2b the sample has been tilted by arctan ($1/\sqrt{2}$) $\approx$ 35.2° so that the incident beam was parallel to NiAl[111]. The strong diffraction spots in these images are spots of the NiAl substrate. Due to the different experimental geometries in parts a and b of Figure 2, different diffraction patterns of the substrate are observed. In Figure 2a the rectangular pattern of NiAl(110) shows up and in Figure 2b the hexagonal pattern of NiAl(111) is recognized. Parts a and b of Figure 2 also exhibit diffraction spots due to the palladium clusters which are marked by arrows. The hexagonal symmetry of the Pd(220) type spots in Figure 2a demonstrates that the (111) directions of the palladium clusters are parallel to the surface normal (Pd[111]||γ-Al$_2$O$_3$[111]||NiAl[110]). From the azimuthal orientation of the spots it follows that the azimuthal orientation of the Pd lattice is Pd[1$\bar{1}$0]||NiAl[1$\bar{1}$0]. The angular misalignment is typically less than 2°.

In Figure 2b the Pd clusters are illuminated along their [110] directions. The palladium spots are of 111 type (marked by "→"), 200 type ("⇒") and 220 type ("≡>") as expected for 111-oriented clusters.

TEM images taken in the same experimental geometries as the diffraction patterns in parts a and b of Figure 2 are displayed in parts a and c of Figure 3. In both figures the orientation of the substrate lattice is indicated. Pd clusters on the surface are characterized by well-developed moiré fringes that result from double diffraction involving a reciprocal lattice vector of the NiAl substrate and another one of the Pd cluster under consideration. The insets display single clusters on an expanded scale. Due to the different illumination angles in parts a and c of Figure 3, different types of moiré fringes are observed on the Pd clusters. Fringes in Figure 3a involve diffraction spot pairs of NiAl(111) and Pd(220) type whereas in Figure 3c the fringes are of NiAl(110)/Pd(200) and NiAl(110)/Pd(111) type. The inset in Figure 3c displays a cluster where both types of fringes are visible at the same time. In parts b and d of Figure 3, the formation of fringes is illustrated in reciprocal space. Table 1 lists the observed types of fringes.

Assuming that the lattices of the clusters are not distorted too much by the interaction with the substrate, we have calculated the lattice constants and the nearest neighbor distances within the clusters as a function of the cluster size from the fringes (for details of the calculation see ref 18). Clusters with all three types of fringes listed in Table 1 have been taken into account. The result is displayed in Figure 4. These data show that the lattice constant decreases with cluster size with the highest observed reduction being 5% for a cluster with a diameter of 12 Å. The reason for this finding is that for small clusters the surface energy is a notable part of the total energy so that it is able to influence the lattice constant. In a simple

Figure 2. Electron diffraction patterns of γ-Al$_2$O$_3$ on NiAl(110) covered with Pd clusters. For panel a the electron beam was oriented along the NiAl[110] direction whereas for panel b it was oriented along NiAl[111]. Some of the palladium induced diffraction spots in panel b are shown with enhanced contrast in the insets in the upper part of the figure. $\Theta_{Pd} = 1$ monolayer.

Figure 3. (a, c) TEM images of γ-Al$_2$O$_3$ on NiAl(110) covered with Pd clusters. In the insets the marked regimes are shown on an expanded scale. (b, d) Schematic drawings showing the reciprocal lattices of the NiAl substrate and the Pd clusters. The orientations of the lattices correspond to the insets in a and c. Key: (a, b) electron incidence as in Figure 2a; (c, d) electron incidence as for Figure 2b. $\Theta_{Pd} = 1$ monolayer.

picture a reduced lattice constant is to be expected for small clusters since the number of bonding partners for the atoms at the surface is smaller than for the bulk atoms. In general, this leads to an increased strength of the remaining bonds between the surface atoms, giving rise to a reduced equilibrium distance at the surface. This induces a surface tension which compresses the bulk. Since this mechanism works more effective for small clusters, a decrease of the lattice constant with decreasing cluster size is to be expected. Calculations for palladium clusters on this topic may be found in refs 8−11. In the present

case the situation is somewhat more complicated. As discussed later in the text, the clusters are covered by a thin oxide film so that the surface does not consist of pure palladium but of a thin oxide film with unknown structure. Additionally, the oxide/substrate bond has to be considered. Therefore additional investigations are needed in order to discuss the obtained results quantitatively.

Modified lattice constants may have a strong impact on the chemical activity. In the case of reduced lattice constants in general an enhanced dispersion bandwidth of the valence bands is to be expected whereas an increased
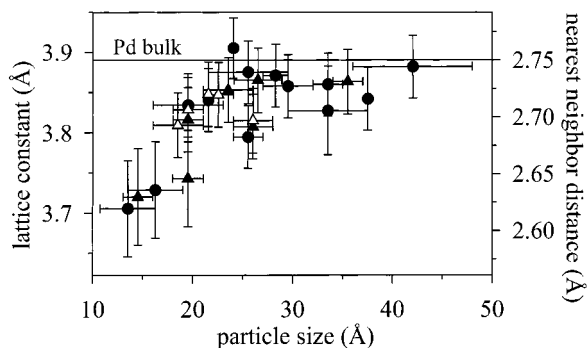
Figure 4. Atomic spacings in Pd clusters on γ-Al$_2$O$_3$/NiAl-(110) as a function of the cluster size. Filled circles are derived from moiré fringes of type 1 in Table 1. Filled triangles correspond to type 2 and open triangles to type 3. The horizontal bars illustrate the difference of the lengths and the widths of the clusters whereas the vertical bars are estimated errors.

lattice constant will lead to reduced dispersion. Also a shift of the center of the valence bands may occur. Nørskov and co-workers[19,20] have calculated the valence band structure and the strength of interaction with CO for a strained Fe(110) overlayer on W(110) (lattice constant increased by 10%). The center of the Fe 3d bands was calculated to be shifted by 0.40−0.46 eV to smaller binding energy, which resulted, according to the calculations, in an enhanced strength of the CO−metal bond due to an increased Fe 3d → π* charge transfer. For an N$_2$ adsorbate on these films a stronger bonding and a significantly enhanced tendency toward dissociation were found experimentally.[21] Here also an increased Fe 3d → π* charge transfer may be responsible for this result.

In the case of small particles, even stronger deviations of the electronic structure from that of the bulk material may occur. The electronic structure of very small clusters may not be described in a band structure picture; here a description in terms of molecular levels is more appropriate. The levels will depend strongly on the shape and size of the clusters, and therefore a strong dependence of the catalytic activity on the cluster size is to be expected. For gold particles supported on titania the catalytic activity for CO oxidation has been studied as a function of cluster size.[22] It was found that the activity of the otherwise rather unreactive gold particles exhibits a strong maximum for a cluster size of about 2.8 nm which was attributed to the appearance of nonmetallic properties for cluster sizes below 3.5 nm. For the same catalytic reaction a size effect has also been reported for Pd clusters deposited on MgO-(100).[23] A study of the electronic properties of small Pd particles deposited on Al$_2$O$_3$/Re(0001) as a function of cluster size revealed that in this case a metal to nonmetal transition occurs at a cluster size of about 2.5 nm.[24]

The observed trend for Pd clusters (see Figure 4) is in line with results obtained for Pt and Ta clusters on γ-Al$_2$O$_3$-(111)/NiAl(110).[1,2] However, for Pt clusters the observed decrease was larger (10%).[1] This may be traced back to the different shapes of Pd and Pt clusters: Pd clusters are

not as flat as Pt clusters.[14,25] This means that the shape of the Pd clusters is mainly determined by surface tension whereas the substrate/cluster interaction has a substantial influence on the shape of Pt clusters. Thus the less pronounced decrease of the lattice constant of Pd clusters may be due to the weaker cluster/substrate interaction. Another point to note is that the number of surface and interface atoms relative to the total number of atoms is larger for flat clusters which may also give rise to a more pronounced lattice contraction as observed for Pt clusters.

It is known that palladium clusters tend to form multiply twinned particles (MTP)[26−29] when the coupling to the substrate is weak. Such particles are characterized by a 5-fold symmetry which is not found for bulk material. They exhibit decahedral or icosahedral shapes and consist of five tetrahedrons with common edges and 20 tetrahedrons with common vertexes. Although tetrahedrons cannot be closely packed into a decahedron or icosahedron, no gaps are observed in the structure due to a elastic lattice deformation which increases from the center to the periphery.[30,31] The substrate/cluster interaction is weaker for Pd clusters on γ-Al$_2$O$_3$/NiAl(110) than for Pt clusters. Nevertheless, it is strong enough to prevent MTP formation as concluded from the palladium induced intensity in Beugungsbildera. This intensity exhibits a 6-fold symmetry which is not possible for Pd−MTP particles.

In contrast to the result presented here, some studies report that the lattice constant of Pd clusters increases with decreasing cluster size.[13,32,33] This contradiction may be due to MTP particles formed in the studied systems since the atomic density in such particles is smaller than in the bulk material. When clusters are not prepared under UHV conditions, MTP formation is more likely, since in this case the substrate surface may be contaminated (OH groups, etc.) which may reduce the substrate/cluster interaction significantly. In the present case no OH groups are on the surface of the oxide so that there is a direct cluster−oxide interaction. This interaction is not negligible as concluded from previous studies under UHV conditions.[4,14,15]

From the different types of moiré fringes, different distances within the palladium lattice have been calculated (see Table 1). Type 1 yields a distance in the 110 direction, type 2 one in the 100 direction and type 3 one in the 111 direction. From these distances the lattice constant was calculated assuming a basically nondistorted fcc lattice. If this condition were not fulfilled, different values for the lattice constants calculated from different types of fringes would result. The data displayed in Figure 4 show that the lattice constants calculated from different types of fringes agree well within the limits of the experimental error, indicating that the anisotropy of the lattice contraction is small.

The lattice orientation of Pd clusters on unsupported Al$_2$O$_3$ seems to be basically the same as on supported alumina. Unsupported alumina forms at the boundary of

(19) Hammer, B.; Morikawa, Y.; Nørskov, J. K. *Phys. Rev. Lett.* **1996**, *76*, 2141.

(20) Ruban, A.; Hammer, B.; Stoltze, P.; Skriver, H. L.; Nørskov, J. K. *J. Mol. Catal. A* **1997**, *115*, 421.

(21) Homann, K.; Kuhlenbeck, H.; Freund, H.-J. *Surf. Sci.* **1995**, *327*, 216.

(22) Valden, M.; Lai, X.; Goodman, D. W. *Science* **1998**, *281*, 1647.

(23) Becher, C.; Henry, C. R. *Surf. Sci.* **1996**, *352*, 457.

(24) Cai, Y. Q.; Bradshaw, A. M.; Guo, Q.; Goodman, D. W. *Surf. Sci.* **1998**, *399*, L357.

(25) Libuda, J.; Bäumer, M.; Freund, H.-J. *J. Vac. Sci. Technol. A* **1996**, *12*, 1.

(26) Hofmeister, H. *Z. Phys. D* **1991**, *19*, 307.

(27) Allpress, J. G.; Sanders, J. V. *Surf. Sci.* **1967**, *7*, 1.

(28) Ogawa, S.; Ino, S. *J. Cryst. Growth* **1972**, *13/14*, 48.

(29) Renou, A.; Gillet, M. Observation of decahedral and icosahedral structures in platinum and palladium particles. In *Proceedings 2nd International meeting on small particles and inorganic clusters*; Oxford University Press: Lausanne, Switzerland, 1980.

(30) Nepijko, S. A. *Physical properties of small metallic particles*; Naukova Dumka: Kiev, USSR, 1985 (in Russian).

(31) Nepijko, S. A.; Stypkin, V. I.; Hofmeister, H.; Scholtz, R. *J. Cryst. Growth* **1986**, *76*, 501−506.

(32) Heinemann, K.; Poppa, H. *Surf. Sci.* **1985**, *156*, 265−274.

(33) Jacobs, J. W. M.; Schryvers, D. *J. Catal.* **1987**, *103*, 436.
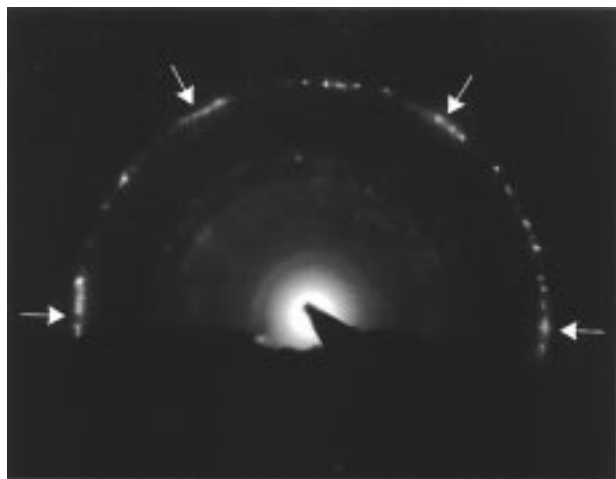
Figure 5. Electron diffraction pattern of Pd clusters on unsupported alumina. $\Theta_{Pd} = 1$ monolayer.

the hole in the sample where the substrate is so thin that it is fully oxidized during the oxidation process.[18] Figure 5 shows a diffraction pattern of palladium clusters on unsupported oxide displaying Pd-induced intensity with 6-fold symmetry. This demonstrates that the Pd clusters on unsupported alumina are also (111) oriented. No obvious signs of MTP formation are observed.

Chemical Composition of the Pd Clusters

The prepared samples were transferred through air from the UHV chamber to the microscope. Therefore one might expect that the clusters are oxidized. However, the diffraction patterns (parts a and b of Figure 2) as well as the calculated lattice constants (Figure 4) do not support this expectation. No spots due to the lattices of PdO or PdO_2 were observed in the diffraction data. To obtain information on the chemical state of the palladium clusters, XPS spectra were recorded. The two peaks in the spectra displayed in Figure 6 are to be attributed to the Pd $3d_{5/2}$ and Pd $3d_{3/2}$ levels. According to the literature data, the binding energies of the levels are 335.2 and 340.5 eV, respectively, for bulk palladium with an energetic spacing of 5.3 eV.[34] The energetic spacing of the levels is the same in Figure 6 although the peaks are shifted by about 0.8 eV to higher energy. There are two possible reasons for this shift.

1. According to ref 35, electron binding energies of small particles on electrically nonconducting substrates may shift to higher binding energy due to the limited space available for charge delocalization.

2. For bulk PdO and PdO_2 the binding energies of the Pd3d levels are shifted by 1 and 2.5 eV, respectively, toward higher energy.[36]

The existing TEM data exclude the formation of fully oxidized clusters. However, it could be the case that the clusters are oxidized at their surface. To check this the sample has been bombarded with He$^+$ ions. The data presented in Figure 6 demonstrate that neither removal of one Pd layer nor removal of three Pd layers leads to a
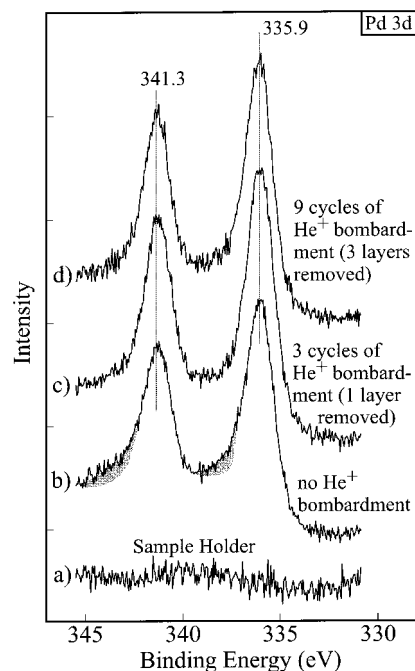
(34) Fuggle, J. C.; Mårtensson, N. *J. Electron Spectrosc. Relat. Phenom.* **1980**, *21*, 275.

(35) Bäumer, M.; Libuda, J.; Freund, H.-J. Metal Deposits on Thin Well Ordered Oxide Films: Morphology, Adsorption and Reactivity. In *Nato Advanced Study Institute, NATO ASI Series E*; Lambert, R. M., Pacchioni, G., Eds.; Kluwer Academic Press: Dordrecht, The Netherlands, 1997; Vol. 331.

(36) Moulder, J. F.; Stickle, W. F.; Sobol, P. E.; Bomben, K. D. In *Handbook of X-ray photoelectron Spectroscopy*; Chastain, J., Ed.; Perkin-Elmer: Eden Prairie, MN, 1992.

Figure 6. XPS spectra of palladium clusters on γ-Al$_2$O$_3$/NiAl-(110). Before spectra c and d were taken the sample was bombarded with He$^+$ ions. One cycle corresponds to 3 min of bombardment with ions with a kinetic energy of 1000 eV and a current density at the sample surface of about 6 μA/cm^2. Θ_{Pd} = 1 monolayer.

shift of the main peaks. However, some weak intensity in spectrum b (shaded areas) is not found in the spectra taken after ion bombardment (parts c and d). The energy separation of the shaded intensity and the main peaks is about 2.5 eV pointing toward formation of a thin oxide layer with PdO_2 stoichiometry. Its thickness corresponds to no more than one layer since the oxide induced intensity has disappeared after removal of one layer by sputtering (Figure 6c).

Summary

Using TEM and XPS we have studied palladium clusters deposited onto a well-ordered Al$_2$O$_3$ film grown by oxidation of NiAl(110). The TEM data reveal that the lattice constant of the clusters decreases with decreasing cluster size. Within the limits of the experimental error this effect is isotropic. The highest observed reduction of the lattice constant is about 5% for a cluster with a diameter of 12.5 Å. This is smaller than the corresponding value for Pt clusters,[1] which may at least partly be due to the different cluster shapes.

The palladium clusters grow epitaxially on the substrate with Pd[111]||NiAl[110] and Pd[1$\bar{1}$0]||NiAl[1$\bar{1}$0]. This is the same orientation as found previously for Pt clusters.[1]

Similar to tantalum and platinum clusters on Al$_2$O$_3$/NiAl(110),[1,2] palladium clusters also appear to be quite inert with respect to oxidation. Only a thin oxide film with a thickness of less than a monolayer is formed.